

Pentadecaibins I–V: 15-Residue Peptaibols Produced by a Marine-Derived *Trichoderma* sp. of the *Harzianum* Clade

Anne-Isaline van Bohemen, Nicolas Ruiz,* Aurore Zalouk-Vergnoux, Aurore Michaud, Thibaut Robiou du Pont, Irina Druzhinina, Lea Atanasova, Soizic Prado, Bernard Bodo, Laurence Meslet-Cladiere, Bastien Cochereau, Franck Bastide, Corentin Maslard, Muriel Marchi, Thomas Guillemette, and Yves François Pouchus



Cite This: <https://dx.doi.org/10.1021/acs.jnatprod.0c01355>



Read Online

ACCESS |



Metrics & More

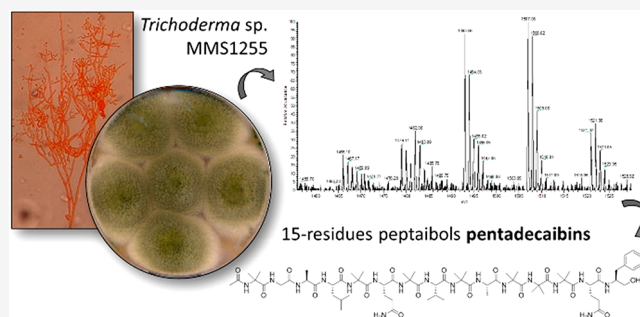


Article Recommendations



Supporting Information

ABSTRACT: In the course of investigations on peptaibol chemodiversity from marine-derived *Trichoderma* spp., five new 15-residue peptaibols named pentadecaibins I–V (1–5) were isolated from the solid culture of the strain *Trichoderma* sp. MMS1255 belonging to the *T. harzianum* species complex. Phylogenetic analyses allowed precise positioning of the strain close to *T. lentiforme* lineage inside the *Harzianum* clade. Peptaibol sequences were elucidated on the basis of their MS/MS fragmentation and extensive 2D NMR experiments. Amino acid configurations were determined by Marfey's analyses. The pentadecaibins are based on the sequences Ac-Aib¹-Gly²-Ala³-Leu⁴-Aib/Iva⁵-Gln⁶-Aib/Iva⁷-Val/Leu⁸-Aib⁹-Ala¹⁰-Aib¹¹-Aib¹²-Aib¹³-Gln¹⁴-Pheol¹⁵. Characteristic of the pentadecaibin sequences is the lack of the Aib-Pro motif commonly present in peptaibols produced by *Trichoderma* spp. Genome sequencing of *Trichoderma* sp. MMS1255 allowed the detection of a 15-module NRPS-encoding gene closely associated with pentadecaibin biosynthesis. Pentadecaibins were assessed for their potential antiproliferative and antimicrobial activities.



Numerous fungi belonging to the genus *Trichoderma* are known to produce bioactive linear nonribosomal peptides (NRPs) named peptaibols. Peptaibols are characterized by molecular masses ranging from 500 to 2000 Da containing 5–20 amino acid (AA) residues, an *N*-acetyl terminus, and a *C*-terminal AA reduced into the corresponding amino alcohol.^{1–4} Peptaibol biosynthesis by nonribosomal peptide synthetases (NRPSs)^{5–7} allows incorporation of nonproteinogenic AAs into the chain such as α -amino-isobutyric acid (Aib) or isovaline (Iva).² In *Trichoderma* spp., peptaibols are produced as complex microheterogeneous mixtures and can be classified into five main families (11-, 14-, 18-, 19-, and 20-residue peptaibols) according to their AA chain length. Peptaibols represent the most important subgroup of the peptaibiotics group, and numerous sequences have already been published and listed in the Comprehensive Peptaibiotics Database.^{8,9}

Peptaibols have been studied for their potential biological activities particularly as alternative sources for antibiotic research or as new therapeutic agents.^{10,11} Indeed, they have been shown to exhibit a wide range of biological activities including antibacterial activity against Gram-positive bacteria^{12–15} and dormant mycobacteria,^{16,17} antifungal activity,^{14,18,19} antiviral activity, particularly against infection caused

by the tobacco mosaic virus,^{20–22} and antiparasitic activity against amebae (*Dictyostelium* sp.)²³ and protozoa (*Plasmodium falciparum*).²⁴ They have been also studied for their activities against fungal plant pathogens.^{25–28} Peptaibols are known to act by forming pores or voltage-dependent ion channels in cell membranes, increasing membrane permeability.^{23,29}

In a continuation of our investigations into peptaibol chemodiversity of French marine-derived *Trichoderma*,^{30–33} we focused in this study on the peptaibol production of the strain *Trichoderma* sp. MMS1255. Phylogenetic analysis was performed to determine the precise taxonomic position of the peptaibol-producing strain within the *Trichoderma* genus and more specifically in the *T. harzianum* species complex. Peptaibols isolated contained 15 AA and were characterized by the lack of the widespread Aib-Pro motif. Their sequences

Received: December 17, 2020

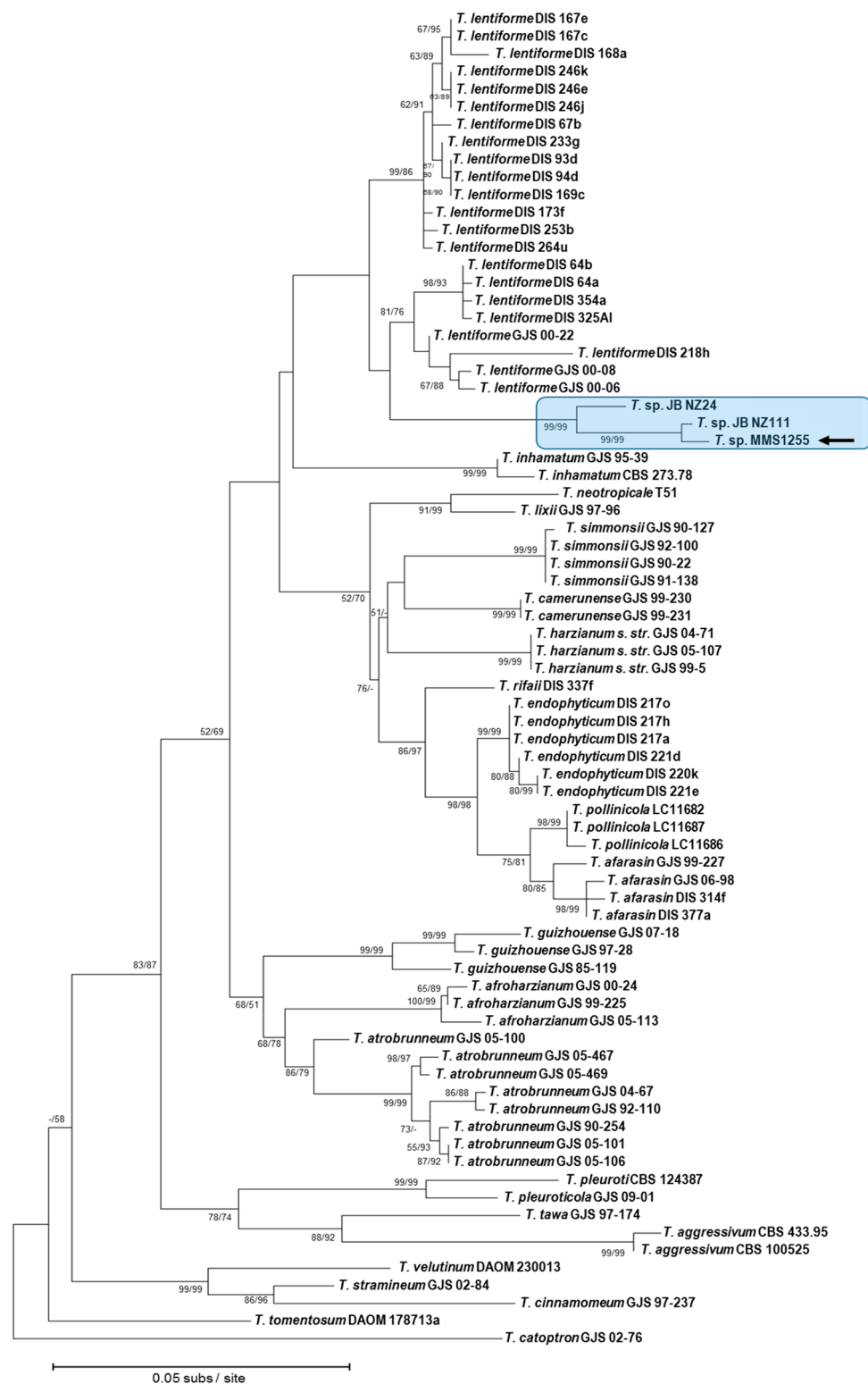
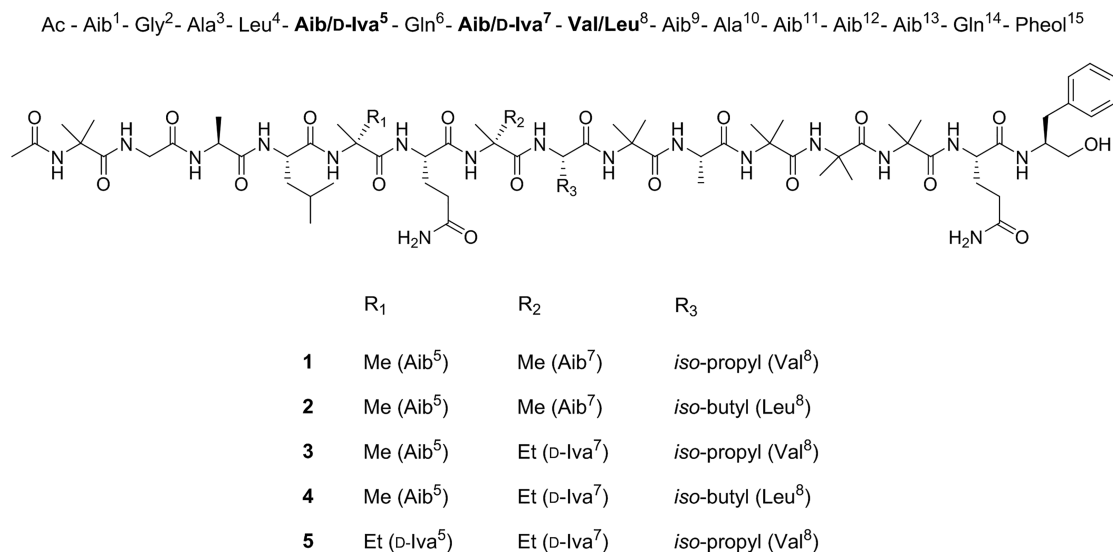


Figure 1. Phylogram of the best maximum likelihood tree (log likelihood: -4619.24) of *tef1* and *cal*, which includes only species in the *T. harzianum* complex. Values at nodes represent ML bootstrap (MLBP)/MP bootstrap (MPBP). The tree is drawn to scale, with branch lengths measured in the number of substitutions per site. The analysis involved 76 nucleotide sequences. There were a total of 734 positions in the final data set. Evolutionary analyses were conducted in MEGA7.³⁸

were determined by MS analysis, and their complete structures were established by NMR spectroscopy. Marfey analysis and circular dichroism were used for the determination of the AA configurations. The genome sequencing of the peptaibol-producing strain revealed the presence of a new gene encoding

a 15-module NRPS. The organization of modules and domains in this gene has never been described before and may be involved in the biosynthesis of the isolated peptaibols. Cytotoxicity and antimicrobial activities were shown for these new compounds.

Chart 1



RESULTS AND DISCUSSION

Morphological and Phylogenetic Analyses of *Trichoderma* sp. MMS1255. The dextrose casein agar (DCA) culture of strain MMS1255 was observed as successive concentric greenish to whitish zones on the agar plate surface. Microscopically, typically highly branched conidiophores were observed producing clustered phialides arising near 90° with respect to the other members (Figure S1). The taxonomic identification was performed by DNA barcoding (Table S1, Figure S2). Preliminary molecular identification based on the internal transcribed spacer regions of the nuclear rRNA gene cluster (ITS1 and ITS2) led to the *Trichoderma harzianum* species complex. However, ITS is not sufficiently polymorphic to distinguish species in the *T. harzianum* complex;³⁴ thus we used the translation elongation factor 1- α (*tef1*) and RNA polymerase II subunit 2 (*rpb2*) gene markers. This analysis localized the strain *Trichoderma* sp. MMS1255 among the *Trichoderma harzianum* Clade (Figure S2).³⁵ For a deeper identification inside this infrageneric group, we performed a combined analysis of the marker genes *tef1* and calmodulin (*cal*). This resulted in the identification of the strain MMS1255 close to the *T. lentiforme* lineage and to two isolates previously described as *T. harzianum* JBNZ24 and JBNZ111 (Figure 1).³⁶ Considering the genealogical concordance phylogenetic species recognition (GCPSR) concept,³⁷ further phenotyping characterizations are needed to clarify *Trichoderma* sp. MMS1255 and *T. harzianum* JBNZ24 and JBNZ111 phylogenetic localization within or outside the borders of *T. lentiforme*.

Isolation and Structure Elucidation of Pentadecabins (1–5). A peptaibol-enriched fraction extracted from a solid culture (DCA) of *Trichoderma* sp. MMS1255 was analyzed by MS and revealed the presence of an unusual MS profile with $[M + Na]^+$ ions ranging from m/z 1466 to 1521 (Figure S3). Whereas ions ranging from m/z 1466 to 1493 were supposed to correspond to 14-residue peptaibols produced by *Trichoderma* strains,^{5,26,39,40} ions m/z 1493 and 1521 did not match any known peptaibols. Herein, we report the discovery, structure elucidation, and biological activities of five 15-residue peptaibols (1–5) isolated from the marine-derived strain *Trichoderma* sp. MMS1255.

Compound 1 was obtained as a white powder. The molecular formula was determined to be C₆₈H₁₁₃N₁₇O₁₈ on the basis of HRESIMS (m/z 750.9132 $[M + 2Na]^{2+}$). The amino acid sequence of 1 was determined on the basis of ESIMS² analyses by identifying fragment ions of the series a_n, b_n, y_{nP} generated in positive ionization (P refers to positive-ion mode) and y_{nN} generated in negative ionization (N for negative-ion mode) (Figure 2, Table S2). Fragmentation of the sodium adduct $[M + Na]^+$ produced a series of fragment ions a₅/b₅ to a₁₄/b₁₄, providing successive losses of Gln⁶, Aib⁷, Vxx⁸, Aib⁹, Ala¹⁰, Aib¹¹, Aib¹², Aib¹³, Gln¹⁴, and the C-terminal Pheol¹⁵ (phenylalaninol; Vxx = Val or Iva). In order to complete the sequence, ESIMS² fragmentation of the deprotonated molecule $[M - H]^-$ yielded diagnostic fragment ions y_{4N} to y_{14N}. Hence, the N-terminal part of the sequence was assigned as Ac-Aib¹-Gly²-Ala³-Lxx⁴-Aib⁵-Gln⁶-Aib⁷-Vxx⁸-Aib⁹-Ala¹⁰-Aib¹¹ (Lxx = Leu or Ile). Fragment ions y_{7P} to y_{14P} assigned in positive mode supported the N-terminal sequence deduced from the y_{nN} ions series. Based on the above mass spectrometry analysis, the sequence of 1 was proposed to be Ac-Aib¹-Gly²-Ala³-Lxx⁴-Aib⁵-Gln⁶-Aib⁷-Vxx⁸-Aib⁹-Ala¹⁰-Aib¹¹-Aib¹²-Aib¹³-Gln¹⁴-Pheol¹⁵.

The sequence determined from mass spectral fragmentations was thus verified by 1D and 2D NMR correlations, allowing in addition the assignment of the isomeric residues Val/Iva and Leu/Ile (Figure 3, Table 1).

The ¹H NMR spectrum of compound 1 exhibited in the range 6.7–9 ppm 17 exchangeable signals characteristic of amide protons, among which 11 singlets corresponding to seven Aib residues, two side-chain NH₂ protons of the two Gln, one broad singlet characterizing one Gly, five doublets (for Ala, Leu, two Gln, and Val), and two multiplets (for Ala and Pheol). In addition, the aromatic protons of the monosubstituted phenyl ring of the Pheol were characterized by multiplets at δ_H 7.13, 7.18, and 7.27. Between δ_H 1.48 and 1.37 ppm were depicted 14 methyl singlets assigned to seven Aib residues.

¹H–¹H correlations from COSY and TOCSY spectra allowed defining seven spin systems corresponding to Gly, two Ala, Leu, Val, and two Gln as represented in Figure 3. An additional moiety was pointed out by ¹H–¹H correlations between a hydroxy group at δ_H 4.53, the

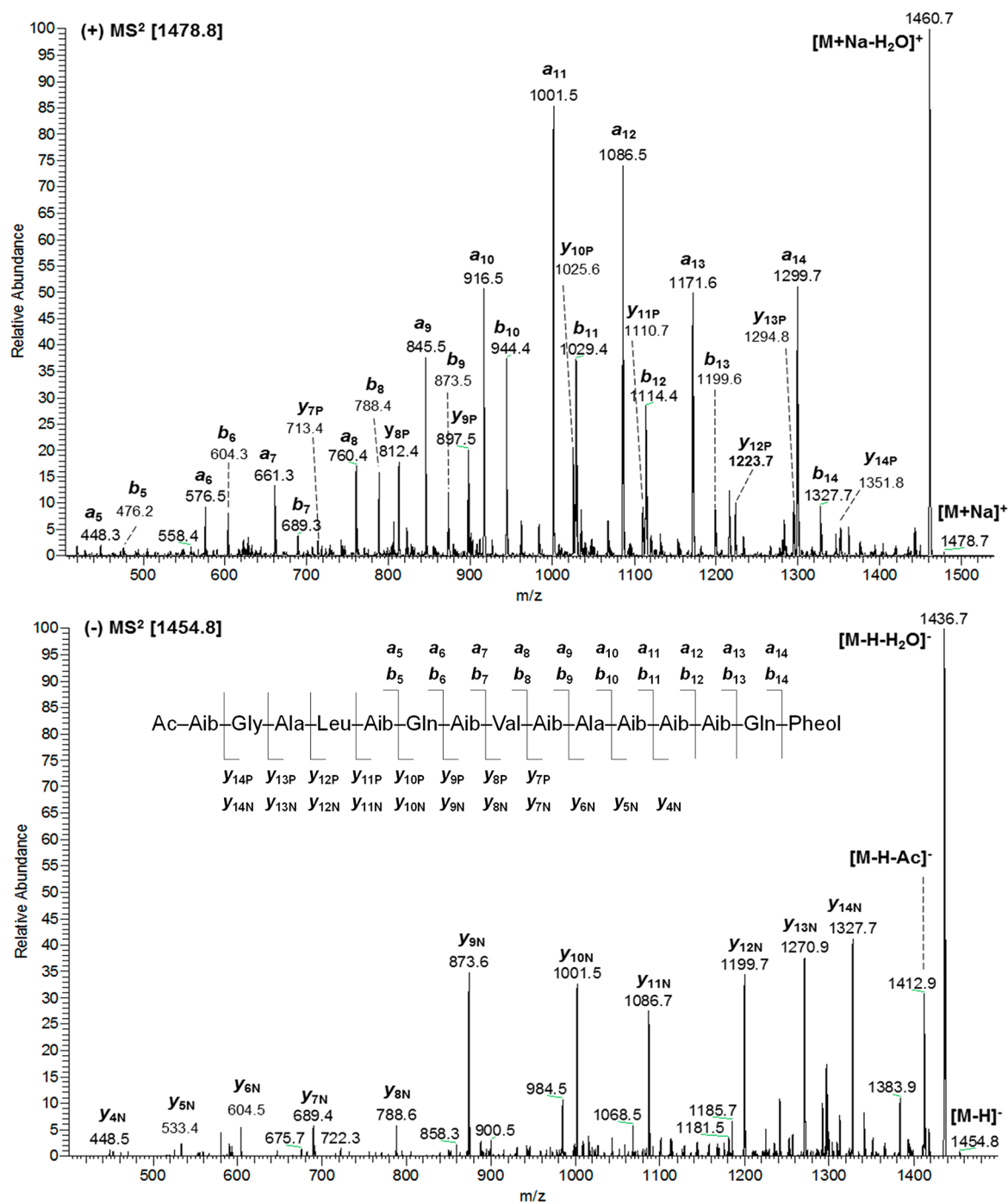


Figure 2. Positive and negative ESIMS² fragmentations of pentadecaibin I (1).

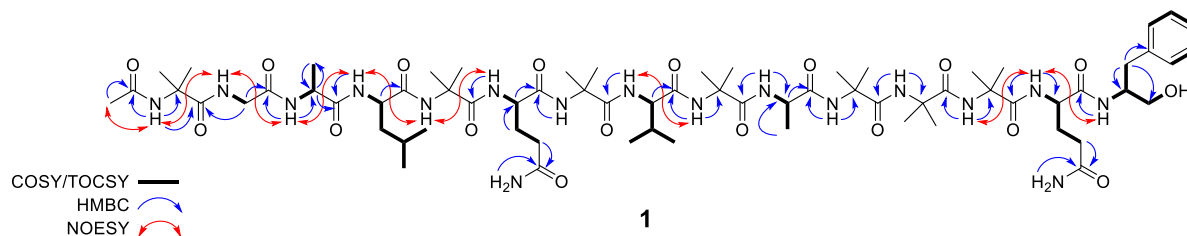


Figure 3. NMR key correlations of pentadecaibin I (1) (COSY/TOCSY, HMBC, and NOESY).

methylene group at δ_{H} 3.37 (δ_{C} 63.2), and the methine at δ_{H} 3.89 (δ_{C} 52.4), which itself was linked to the NH at δ_{H} 7.13

and the methylene at δ_{H} 2.89/2.57 (δ_{C} 36.7). ^1H - ^{13}C HMBC correlations allowed this methylene carbon to be linked to the

The sequences of the other isolated peptaibols were identified and characterized in the same way.

Compound **2** was obtained as a white powder. The molecular formula was determined to be $C_{69}H_{115}N_{17}O_{18}$ on the basis of HRESIMS (m/z 757.9172 [$M + 2Na$] $^{2+}$), indicating the presence of an additional methylene group between **1** and **2**. This was confirmed by positive and negative mass fragmentations (Figures S4 and S5, Table S2), suggesting the presence of Ile/Leu in position 8 instead of Val⁸ for compound **1**. Detailed analyses of 1D and 2D NMR spectroscopic data were consistent with mass fragmentation analyses, and both residues were identified as leucine from COSY and TOCSY data (Table S3). HMBC correlations confirmed the second Leu residue in position 8. Indeed, 1H – ^{13}C correlations were observed between the CO group of the Aib⁷ at δ_C 176.3 and the NH at δ_H 7.89 of the Leu⁸, and the CO group of this Leu at δ_C 174.0 was correlated to the methine H α at δ_H 3.90 (δ_C 54.8) and to the NH at δ_H 8.03 of the Aib⁹ (Figure S27). Therefore, the structure of compound **2** was established as Ac-Aib¹-Gly²-Ala³-Leu⁴-Aib⁵-Gln⁶-Aib⁷-Leu⁸-Aib⁹-Ala¹⁰-Aib¹¹-Aib¹²-Aib¹³-Gln¹⁴-Pheol¹⁵ and named pentadecaibin II.

Compound **3** was obtained as a white powder and exhibited the same molecular formula ($C_{69}H_{115}N_{17}O_{18}$) as compound **2**. On the basis of mass fragmentation analyses, compound **3** only differed from **1** by the presence of a Val/Iva instead of an Aib in position 7 (Figures S6 and S7, Table S2). Mass spectrometry sequencing was confirmed by NMR investigations (Table S4), and the TOCSY spectrum showed characteristic signals of one Iva and one Val isomeric residue. The CO group of Gln⁶ at δ_C 173.1 was correlated to the NH of Iva⁷ at δ_H 7.76 and the CO of Iva⁷ at δ_C 176.6 to the NH of Val⁸ at δ_H 7.74 (Figure S36). Thus, Aib⁷ in compound **1** changed to Iva⁷ in **3**. Compound **3** was identified as Ac-Aib¹-Gly²-Ala³-Leu⁴-Aib⁵-Gln⁶-Iva⁷-Val⁸-Aib⁹-Ala¹⁰-Aib¹¹-Aib¹²-Aib¹³-Gln¹⁴-Pheol¹⁵ and consequently named pentadecaibin III.

Compound **4** was obtained as a white powder. On the basis of HRESIMS studies, the molecular formula $C_{70}H_{117}N_{17}O_{18}$ was deduced from the [$M + 2Na$] $^{2+}$ at m/z 764.9263. Mass fragmentation analyses (Figures S8 and S9) demonstrated that peptide **4** only differs from **3** by the replacement of the Val residue by an Ile/Leu in position 8 (Table S2). Detailed NMR analyses were consistent with mass fragmentation sequencing and revealed that compound **4** only differed from **3** by the presence of two Leu residues instead of one, the presence of an Iva, and the absence of Val (Table S5). The CO of Gln⁶ at δ_C 173.2 was correlated to the NH of the Iva⁷ at δ_H 7.78, the CO of which at δ_C 176.8 was correlated to the NH at δ_H 7.85 of the second Leu, which was thus located at position 8 (Figure S45). Therefore, compound **4** was determined as Ac-Aib¹-Gly²-Ala³-Leu⁴-Aib⁵-Gln⁶-Iva⁷-Leu⁸-Aib⁹-Ala¹⁰-Aib¹¹-Aib¹²-Aib¹³-Gln¹⁴-Pheol¹⁵ and named pentadecaibin IV.

Compound **5** was obtained as a white powder. HRESIMS analyses of the [$M + 2Na$] $^{2+}$ at m/z 764.9180 confirmed that compound **5** exhibits the same molecular formula ($C_{70}H_{117}N_{17}O_{18}$) as compound **4**. Based on mass fragmentation sequencing, three Val or Iva residues were assigned in positions 5, 7, and 8 (Figures S10 and S11, Table S2). NMR investigations confirmed the mass fragmentation and revealed that compound **5** was characterized by the presence of two Iva and one Val (Table S6, Figure S54). The CO of Leu⁴ at δ_C 173.5 was correlated to the NH at δ_H 8.10 of one of the Iva

(Iva⁵). The CO of this Iva at δ_C 176.6 gave a cross-peak in the HMBC spectrum with the NH of Gln⁶ at δ_H 7.80. As the CO of Gln⁶ at δ_C 173.1 was correlated to the NH at δ_H 7.75 of the second Iva (Iva⁷) and the CO of which at δ_C 176.6 was correlated to the NH at δ_H 7.80 of a Val (Val⁸), compound **5** only differed from compound **4** by the replacement of an Aib by an Iva in position 5. Therefore, compound **5** was determined as Ac-Aib¹-Gly²-Ala³-Leu⁴-Iva⁵-Gln⁶-Iva⁷-Val⁸-Aib⁹-Ala¹⁰-Aib¹¹-Aib¹²-Aib¹³-Gln¹⁴-Pheol¹⁵ and named pentadecaibin V.

The solution conformation of pentadecaibins in DMSO- d_6 was tentatively examined by NMR, based on the observed $^3J_{NH,\alpha H}$ coupling constants and the inter-residue NOE connectivities. The $^3J_{NH,\alpha H}$ coupling constant values mainly lower than 7 Hz agreed with a helical structure. The inter-residue NOE patterns observed for the five pentadecaibins (**1**–**5**) on their NOESY spectra were similar, and strong NOE correlations $d_{NN(i, i+1)}$ and $d_{\alpha N(i, i+1)}$ were observed, in agreement with the proposed sequences (Figure 3, Figures S15, S23, S27, S32, S36, S41, S45, S50, and S54). A helical structure was also obvious from the series of NOESY correlations between contiguous residues such as strong $d_{NN(i, i+1)}$, $d_{NN(i+2, i)}$, and $d_{NN(i, i+3)}$. The prevalence of a helix stabilized by 4→1 intramolecular hydrogen bonds (3₁₀-helix type) over an α -helix, which is stabilized by 5→1 intramolecular hydrogen bonds, arose from the absence of $d_{NN(i, i+4)}$ and the stronger peaks of $d_{NN(i, i+2)}$ as compared to $d_{NN(i, i+3)}$. As similar conformational results were observed for all five peptaibols, it was concluded that the substitutions Aib → Iva (positions 5 and 7) and Val → Leu (position 8), which were responsible for the microheterogeneity of the pentadecaibins, were without significant influence on their secondary structure.

In addition, on the basis of ECD spectra analyses (Figures S19, S28, S37, S46, and S55), the occurrence of two negative maxima at 210 and 225 nm and a positive maximum near 200 nm confirmed the right-handed helical conformation of the pentadecaibins.⁴¹ In this case, for Iva residues of pentadecaibins III (**3**), IV (**4**), and V (**5**), the large $\Delta\delta_H$ values of 1H chemical shift differences between the diastereotopic β -methylene protons (>0.28 ppm) and the chemical shifts of γ -methyl protons and β -methylene carbons confirmed the presence of D-configured Iva (Table 2).^{42,43}

Table 2. 1H and ^{13}C NMR Parameters of Iva Residues in Pentadecaibins III (**3**), IV (**4**), and V (**5**)

NMR parameter	III (3)	IV (4)	V (5)	
	Iva ⁷	Iva ⁷	Iva ⁵	Iva ⁷
$\Delta\delta_{\beta Hb-\beta Ha}$	0.67	0.66	0.51	0.67
$\delta_H \gamma-CH_3$	0.76	0.76	0.76	0.75
$\delta_C \beta-CH_2$	25.0	24.9	25.0	25.0

Moreover, the absolute configurations of the constituent chiral AA of pentadecaibins I–V (**1**–**5**) were determined after acid hydrolysis and subsequent derivatization of the amino acids with Marfey's reagent (L-FDAA)⁴⁴ (Figures S56–S60). Comparison of the L-DAA derivatives of **1**–**5** with appropriate L- and D-standard AA L-DAA derivatives by reversed-phase LC indicated the presence of L-configured AA for Ala, Val, Leu, Glu (resulting from Gln hydrolysis during Marfey's analysis), and Pheol. Marfey's analyses confirmed the presence of D-configured Iva for compounds **3**–**5**. Consequently, all chiral

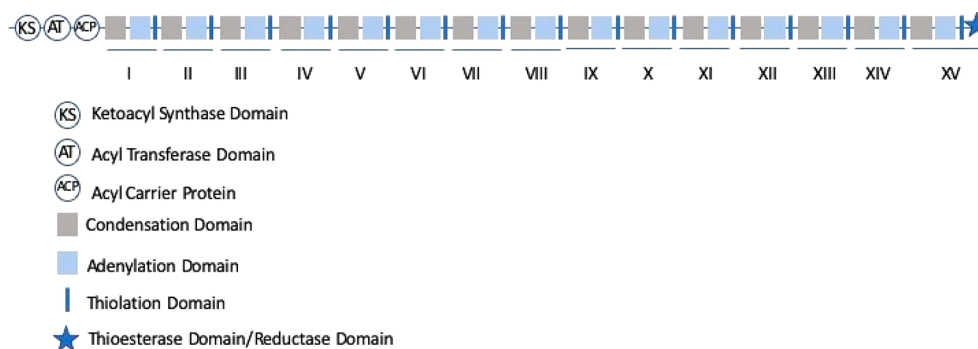


Figure 4. Module organization of the putative NRPS gene encoding the pentadecaibins I–V (1–5). Modules are indicated by numbers I–XV.

Table 3. Prediction of Incorporated AA in Pentadecaibins Based on the Signature Sequences in 15-Module NRPS Adenylation Domains

amino acid position in pentadecaibins	signature sequence in NRPS module ^a	amino acids predicted by NRPS/PKS substrate predictor/NRPSPredictor2 SVM (small cluster prediction) ^b	amino acids detected in pentadecaibins
0	PKS-AT	methylmalonyl-CoA	Ac
1	DLGYLAGVFK	Iva/Val,Leu,Ile,Abu,Iva	Aib
2	DLGiCaVmK	Gly,Ala,Val,Leu,Ile,Abu,Iva/NP ^c	Gly
3	DVGfVAGVlK	Ala/Gly,Ala	Ala
4	DMGFLGGvAK	Val/Val,Leu,Ile,Abu,Iva	Leu
5	DLGivCGVvK	NP ^c /Val,Leu,Ile,Abu,Iva	Aib/Iva
6	DGGMVGGNYK	Gln/Glu,Gln	Gln
7	DAawIVGVvK	Val,Leu,Ile,Abu,Iva/ Val,Leu,Ile,Abu,Iva	Aib/Iva
8	DAFILGgViK	Ala/Val,Leu,Ile,Abu,Iva	Val/Leu
9	DLGYLAGCFK	Iva/Val,Leu,Ile,Abu,Iva	Aib
10	DVGyVAAVYK	Ser/Ser	Ala
11	DLMyFagVAK	Gly,Ala,Val,Leu,Ile,Abu,Iva/NP ^c	Aib
12	DLGFLAGVFK	Iva/Val,Leu,Ile,Abu,Iva	Aib
13	DLGLLAGLfk	Iva/Val,Leu,Ile,Abu,Iva	Aib
14	DGGMVGGNYK	Gln/Glu,Gln	Gln
15	DgFVIAGicK	NP ^c /Pheol,Tripol	Pheol

^aShown in the single-letter amino acid code. ^bShown in the three-letter amino acid code. ^cNP: no prediction.

AAs present in pentadecaibins I–V possess the L-configuration except for the Iva residues (D-configuration).

This is the first report of the description of 15-residue peptaibols within the genus *Trichoderma*. These peptaibols are characterized by the lack of the highly conserved Aib-Pro motif, which is generally characteristic for peptaibols produced by *Trichoderma* spp. Ampullosporins, chalciporins, and tylopeptins, 15-residue peptaibols produced by *Sepedonium* species, are also characterized by the absence of the Aib-Pro motif.^{45–49} However, these peptaibols exhibit sequence patterns that remain different from pentadecaibins.

Interestingly, no 18-residue peptaibols could be detected in *Trichoderma* sp. MMS1255 strain extracts, whereas *Trichoderma* species belonging to the *T. harzianum* complex are known to produce these peptaibol series.^{5,7} Comparison of new 15- and already known 18-residue patterns produced by various *T. harzianum* strains showed a complete sequence similarity with an absence of a 3 AA sequence (Aib¹²-Pro¹³-Leu¹⁴) (Figure S61). *Trichoderma* sp. MMS1255 genome sequencing was performed in order to identify the putative NRPS gene encoding the pentadecaibins.

Genome Sequencing and NRPS Gene Analysis. The genome was sequenced with the PacBio technology. We obtained 228 contigs, and the genome assembly size was estimated at 38.7 Mbp, which is coherent with the size of the other fungi within the *T. harzianum* complex.⁵⁰ All sequences

were submitted to the AntiSMASH software pipeline.⁵¹ Interestingly, only one NRPS gene encoding a 15-module protein was identified in the genome, estimated to be 53.5 kbp (Figure 4).

The presence of ketoacyl synthase and acyltransferase domain genes before the first module gene was consistent with the typical N-terminal acetylation of peptaibols. The latest domain in the gene corresponds to a thioesterase or reductase domain. This domain catalyzes the reduction of the acyl thioester into its primary alcohol via the aldehyde intermediate,⁵² which is in agreement with the typical C-terminal amino alcohol of peptaibols. This NRPS-encoding gene analysis was completed by the prediction of incorporated AA based on the 10 AA signature sequences in the adenylation domains of NRPS modules based on both NRPS/PKS Substrate Predictor and NRPSPredictor2 SVM (Table 3).^{53,54}

All signatures in the adenylation domains were consistent with the AA sequences of pentadecaibins I–V. Based on these results, it can be assumed that pentadecaibins are synthesized by a 15-module NRPS. This is the first detection of a 15-module peptaibol synthetase gene within the *Trichoderma* spp. Contrary to other investigated *Trichoderma* strains within the *T. harzianum* complex, MMS1255 is the only one producing 15-residue peptaibols associated with a 15-module peptaibol synthetase.

Biological Activities of Pentadecaibins. Biological activities of pentadecaibins I–V (1–5) were assessed against cancer cells (KB), Gram-positive (*Staphylococcus aureus*) and negative (*Escherichia coli*) bacteria, and human-pathogenic yeast (*Candida albicans*) (Table 4).

Table 4. Biological Activities of Pentadecaibins I–V (1–5)

compound	cytotoxicity, IC ₅₀ (μ M)	antimicrobial activity, MIC (μ g/ mL)		
	KB cells	<i>S. aureus</i>	<i>E. coli</i>	<i>C. albicans</i>
1	2.4 \pm 0.1	25 \pm 0	>100	>100
2	4.3 \pm 1.1	>100	>100	>100
3	0.8 \pm 0.5	25 \pm 0	>100	>100
4	0.8 \pm 0.2	>100	>100	>100
5	0.7 \pm 0.2	25 \pm 0	>100	>100
Alm F50/5 ^a	9 \pm 1	n.t. ^b (12.5) ^c	n.t.	n.t.

^aSynthetic alamethicin F50/5. ^bn.t., not tested. ^cValue from ref 56.

The cytotoxic activities of the pentadecaibins were consistent with previous reports of cell growth inhibitory activity of 11- and 20-residue peptaibols from a marine-derived *T. longibrachiatum* strain.^{30,32} Pentadecaibins III–V (3–5) incorporating a D-Iva⁷ residue instead of Aib⁷ exhibited higher growth inhibitory activity against KB cells than pentadecaibins I and II (1 and 2). Interestingly, similar observations were obtained with trichodermites A–E assessed on SW620 human colorectal carcinoma cells.⁵⁷ Pentadecaibins did not exhibit noticeable growth inhibition against Gram-negative *E. coli* or the yeast *C. albicans*. However, moderate antibacterial activity against *S. aureus* was observed for pentadecaibins I (1), III (3), and V (5) with MIC values of 25 μ g/mL, being in agreement with previous observations in the literature for antimicrobial activity.^{30,56}

In conclusion, in this study we have identified a new series of 15-residue peptaibols named pentadecaibins I–V (1–5). They are produced by a marine-derived strain belonging to the *harzianum* clade. The phylogenetic position of *Trichoderma* sp. MMS1255 within the *Trichoderma* genus was studied using sequence alignment of combined genes of representative *Trichoderma* strains. No precise identification can be proposed, but the phylogenetic analysis clearly demonstrates the relation of *Trichoderma* sp. MMS1255 to the *T. lentiforme* lineage. The pentadecaibins discovered differ between them by AA exchange in positions 5 (Aib/Iva), 7 (Aib/Iva), and 8 (Val/Leu). They are all characterized by the lack of the Aib-Pro motif widespread in peptaibols produced by *Trichoderma* spp. Genome sequencing allowed the identification for the first time within *Trichoderma* spp. of a 15-module peptaibol synthetase encoding gene closely related to pentadecaibin biosynthesis, according to the prediction of the incorporated AA. The pentadecaibins exhibit moderate cytotoxicity on KB cells and antibacterial activity against *S. aureus*.

EXPERIMENTAL SECTION

General Experimental Procedures. The specific rotation was measured with a PerkinElmer model 341 polarimeter at 589 nm. UV spectra were obtained from a Shimadzu 1605 UV/visible spectrophotometer, at room temperature, over a wavelength range of 200–400 (peptaibols 0.1 mM, MeOH). ECD experiments were carried out using a Jasco J-810 CD spectropolarimeter. Spectra were recorded at room temperature over a wavelength range of 195–260 nm using a 0.2 cm path length cuvette (peptaibols 0.1 mM, MeOH). Measure-

ments were performed using a step scan scanning mode with a data acquisition interval of 0.1 nm, bandwidth of 2 nm, and accumulation of 5. ECD sample spectra are shown after subtracting the baseline, smoothing, and data normalization. IR spectra were recorded on a Shimadzu IR Affinity FTIR spectrometer fitted with an ATR MiRacle 10. One- and two-dimensional NMR spectra were performed on a Bruker Avance III HD 600 MHz spectrometer operating at 600.193 MHz and using a triple-resonance TCI cryoprobe, equipped with shielded gradients z . NMR spectra were recorded in DMSO- d_6 solution and were processed using the Bruker TOPSPIN 3.2 software. Chemical shifts are expressed in δ (ppm) and are referenced to the residual nondeuterated solvent signals (for DMSO- d_6 δ_H 2.49 and δ_C 39.5). For the HMBC experiments the delay (1/2J) was 70 ms, and for the NOESY experiments the mixing time was 500 ms. Mass analyses were carried out using an LCQ electrospray ionization ion-trap mass spectrometer instrument (ESI-IT/MS, Thermo Fisher Scientific) in positive and negative mode with a capillary temperature of 160 °C, capillary voltage of 3.44 V (positive mode) or –9.81 V (negative mode), spray voltage of 4.51 kV, and sheath gas (N_2) flow rate of 19.50 au. Compounds were infused as methanolic solutions (0.5 μ g/mL) directly into the ESI probe with a 500 μ L micrometrically automated syringe (Hamilton) at a flow rate of 3 μ L/min. All spectra were acquired and analyzed by LCQ Xcalibur software (Thermo Fisher Scientific). Total current ion mass spectra (Fullscan mode) were acquired in the range m/z 150 to 2000. Charge state and isotopic distribution were analyzed by a narrow-scan range mode (Zoomscan mode). MS fragmentation was performed by positive and negative ionizations under the same experimental conditions described above for regular MS analysis *via* infusion of methanolic solutions (0.5 μ g/mL). The sodium adduct ions [M + Na]⁺ and the deprotonated molecules [M – H][–] were selected as precursor ions for MS². Peptaibols were sequenced by assignment of the diagnostic fragment ions of the series a_n/b_n and y_{nP} produced in positive-ion mode and y_{nN} produced in negative-ion mode. HRESIMS analyses were conducted using an electrospray ionization ion-trap time-of-flight multistage mass spectrometer (IT-TOFMS, Shimadzu). Organic solvents used for extraction and purification of compounds were purchased from Carlo Erba SDS and distilled prior to use. Water was purified to HPLC-grade quality with a Millipore-QRG ultrapure water system (Millipore). MS analyses were performed using LCMS-grade MeOH (Biosolve). Semi-preparative HPLC purifications and AA Marfey's analysis were carried out on an Agilent 1200 HPLC instrument connected to a corresponding quaternary pump, fraction collector, DAD detector, and Chemstation software. All D- and L-amino acids, Gly, and Aib were purchased from Sigma-Aldrich, except D- and L-Iva, which were purchased from Thermo Fisher Scientific. Acetonitrile (CH₃CN) and trifluoroacetic acid (TFA) used for AA Marfey's analysis were purchased from Carlo Erba and Sigma-Aldrich, respectively.

Isolation, Fungal Strain Identification, and Phylogenetic Analysis. The fungal strain was isolated from marine sediment collected in a shellfish-farming area from the estuary of the river Loire at Port-du-Bec, France. The isolated strain is deposited in the laboratory fungal collection (MMS-Marine Fungal Collection, University of Nantes) under the reference number MMS1255 as well as in the TU Wien Collection of Industrially Important Microorganisms under the reference TUCIM 5509. Strain MMS1255 was identified as belonging to the genus *Trichoderma* on the basis of macroscopic and microscopic morphological features (Figure S1). The identification was completed at the molecular level by amplification and sequencing of internal transcribed spacers and DNA partial sequences of the fourth large intron of translation elongation factor 1- α (*tef1*): RNA polymerase II subunit 2 (*rpb2*) and calmodulin (*cal*). Sequences were deposited in GenBank under accession numbers JQ653081.1, KU758964.1, MN450663.1, and MN428075.1 respectively. Briefly, the mycelium for DNA extraction was grown on potato dextrose agar (PDA) and harvested after 7 days. Genomic DNA was extracted according to the microwave mini-prep procedure described by Goodwin and Lee (1993)⁵⁸ using 100 μ L of lysis buffer (50 mM Tris-HCl pH 7.5, 50 mM EDTA, 3% SDS, 1% 2-

mercaptoethanol). The final DNA pellet was supplemented into 100 μ L of TE buffer (10 mM Tris-HCl pH 8.0, 0.1 mM EDTA) and stored at -20 °C until used. Gene sequences were obtained by polymerase chain reaction (PCR) amplification (GoTaq G2 Hot Start Polymerase, Promega Corporation) and sequenced using Eurofins Genomics facility. DNA partial sequences of *cal*, ITS, *rpb2*, and *tefl* were amplified using the following primers: CAL-228F/CAL-737R,⁵⁹ ITS1/ITS4,⁶⁰ rRPB2-5f/rRPB2-7cr,⁶¹ and EF1-728F⁵⁹/TEF1LLErev,⁶² respectively. ITS sequence (JQ653081) allowed assigning MMS1255 strain to the *Trichoderma* genus. A first phylogenetic analysis aiming to affiliate MMS1255 strain to the *Trichoderma* subclades defined by Jaklitsch and Voglmayr³⁵ was performed using 112 *Trichoderma* spp. combined sequences of *tefl* and *rpb2* (Table S1). For the *Trichoderma* subclade affiliation tree, *Protocrea farinosa* sequences were used as outgroup taxa. A second analysis was performed to determine MMS1255 strain lineages inside the *T. harzianum* clade or to the *T. harzianum* complex defined by Jaklitsch and Voglmayr³⁵ and Chaverri et al.,³⁴ respectively. According to Chaverri et al.,³⁴ *T. catoptron* is one of the more distant species from the *T. harzianum* complex; thus the *T. catoptron* strain GJS 02-76 sequences were used to root phylogenetic trees. For the *Trichoderma* sp. MMS1255 lineage affiliation to the *T. harzianum* complex, the combined sequences of the *tefl* and *cal* genes of 76 representative strains were used (Table S1). As described by Jaklitsch and Voglmayr,³⁵ all alignments were produced with the server version of MAFFT (www.ebi.ac.uk/Tools/mafft), with a gap open penalty of 1.0 and a gap extension penalty in the range of 0.05 to 0.1, with a tree building number = 100 and maxiterate = 100. The resulting alignments were checked and refined using BioEdit version v. 7.0.5.3.⁶³ Maximum likelihood (ML) analysis was performed with MEGA 7.0.26. The general time-reversible model (GTR)⁶⁴ with gamma-distributed substitution rates, additionally assuming a proportion of invariant sites (GTR+I+G), was selected according to the Akaike information criterion (AIC). Initial tree(s) for the heuristic search were obtained automatically by applying neighbor-join and BioNJ algorithms to a matrix of pairwise distances estimated using the maximum composite likelihood (MCL) approach and then selecting the topology with superior log likelihood value. Maximum likelihood bootstrap proportions (MLBPs) were computed with 1000 replicates. Maximum parsimony (MP) trees were obtained by MEGA 7.0.26 using 1000 replicates of heuristic search with random addition of sequences and tree bisection–reconnection (TBR) as the branch-swapping algorithm. All characters were weighted equally. Maximum parsimony bootstrap proportions (MPBPs) were calculated from 1000 replicates, each with 10 replicates of random addition of taxa. Trees were visualized with MEGA 7.0.26 with MLBP and MPBP above 50% as shown at the nodes.

Analytical Cultivation and Peptaibol Profiling by ESI-IT-MS.

For peptaibol chemical profiling, *Trichoderma* sp. MMS1255 was inoculated onto a Petri dish (10 cm diameter) containing 20 mL of marine DCA medium (dextrose 40 g/L, enzymatic digest of casein 10 g/L, agar 15 g/L, Difco, VWR, synthetic sea salt 36 g/L, Reef Crystals, Aquarium Systems). The culture was incubated for 7 days at 27 °C. After incubation, the culture was harvested and mycelia and conidia were scraped from the agar surface. The harvested biomass was extracted by $\text{CH}_2\text{Cl}_2/\text{MeOH}$ (1:2 then 2:1, v/v, 30 mL each) for 30 min at room temperature. The combined extracts were filtered, washed with distilled H_2O (10 mL), and evaporated to dryness to provide an organic extract. The extract was fractionated by vacuum liquid chromatography (VLC) on Chromabond adsorbant (OH) 2 Diol (10 \times 50 mm, 60 \AA , 45 μm , Macherey-Nagel) with $\text{CH}_2\text{Cl}_2/\text{EtOH}$ mixtures (98:2 to 85:15, v/v). The peptaibol-enriched fraction eluting with $\text{CH}_2\text{Cl}_2/\text{EtOH}$ (90:10, v/v) was subjected to ESIMS analysis in infusion mode.

Preparative Cultivation, Extraction, and Purification of Compounds 1–5. Strain MMS1255 was inoculated onto 35 Petri dishes (20 cm diameter) containing 125 mL of marine DCA medium. Cultures were incubated in natural light for 11 days at 27 °C prior to harvesting for biomass extraction, as previously mentioned (see above). After incubation, the harvested biomass was extracted by

$\text{CH}_2\text{Cl}_2/\text{MeOH}$ (1:2 then 2:1, v/v, 1200 mL each) for 2 h at room temperature. The combined extracts were filtered, washed with distilled H_2O (600 mL), and evaporated to dryness to provide an extract (2.8 g). The extract was partitioned in aliquots of 276 mg and fractionated by repetitive VLC, with $\text{CH}_2\text{Cl}_2/\text{EtOH}$ mixtures (98:2, 95:5, 92:8, 90:10, and 85:15, v/v). Peptide-containing fractions ($\text{CH}_2\text{Cl}_2/\text{EtOH}$, 95:5 to 85:15, v/v) were combined to obtain fraction 2 (940 mg) and subjected to liquid chromatography on an open silica gel column (Chromagel, 200 \times 20 mm, 60 \AA , 35–70 μm , SDS), with $\text{CH}_2\text{Cl}_2/\text{MeOH}$ mixtures (100:0 to 80:20, v/v). Fifteen-residue peptaibols were mainly eluted in the 2-9 and 2-10 $\text{CH}_2\text{Cl}_2/\text{MeOH}$ mixtures (85:15, v/v). Chromatographic separation of fraction 2-10 (433 mg) by repetitive reversed-phase preparative HPLC (Luna RP18 column, 250 \times 10 mm, 100 \AA , 5 μm , Phenomenex) yielded five compounds (1–5) eluting respectively in subfractions 2-10-4 to 2-10-8. The mobile phase ($\text{MeOH}/\text{H}_2\text{O}$, 85:15, v/v) was delivered at a constant flow rate of 5 mL/min. Volumes of 900 μL of 10 mg/mL peptaibol solution resuspended in the mobile phase were injected. Detection was performed at 230 nm. All data were acquired by HP ChemStation for LC.

Pentadecaibin I (1): white powder, $[\alpha]_{\text{D}}^{20}$ -21 (c 0.2, MeOH); UV (MeOH) λ_{max} (log ϵ) 204 (3.46) nm; IR ν_{max} 3304, 2929, 1645, 1531, 1454, 1384, 1363, 1294, 1220, 1176, 1043 cm^{-1} ; ^1H and ^{13}C NMR data, Table 1; ESIMS m/z 750.9 $[\text{M} + 2\text{Na}]^{2+}$, m/z 1478.8 $[\text{M} + \text{Na}]^+$; HRESIMS m/z 750.9132 $[\text{M} + 2\text{Na}]^{2+}$ (calcd for $1/2 \text{C}_{68}\text{H}_{113}\text{N}_{17}\text{O}_{18}\text{Na}_2$, 750.9117, Δ 2.0 ppm).

Pentadecaibin II (2): white powder, $[\alpha]_{\text{D}}^{20}$ -17.3 (c 0.34, MeOH); UV (MeOH) λ_{max} (log ϵ) 204 (3.45) nm; IR ν_{max} 3304, 2930, 1649, 1533, 1452, 1384, 1360, 1298, 1225, 1188, 1043 cm^{-1} ; ^1H and ^{13}C NMR data, Table S3; ESIMS m/z 757.9 $[\text{M} + 2\text{Na}]^{2+}$, m/z 1492.8 $[\text{M} + \text{Na}]^+$; HRESIMS m/z 757.9172 $[\text{M} + 2\text{Na}]^{2+}$ (calcd for $1/2 \text{C}_{69}\text{H}_{115}\text{N}_{17}\text{O}_{18}\text{Na}_2$, 757.9195, Δ 3.03 ppm).

Pentadecaibin III (3): white powder, $[\alpha]_{\text{D}}^{20}$ -15.1 (c 1.0, MeOH); UV (MeOH) λ_{max} (log ϵ) 204 nm (3.42) nm; IR ν_{max} 3304, 2935, 1649, 1531, 1456, 1384, 1363, 1290, 1219, 1174, 1043 cm^{-1} ; ^1H and ^{13}C NMR data, Table S4; ESIMS m/z 757.9 $[\text{M} + 2\text{Na}]^{2+}$, m/z 1492.8 $[\text{M} + \text{Na}]^+$; HRESIMS m/z 757.9174 $[\text{M} + 2\text{Na}]^{2+}$ (calcd for $1/2 \text{C}_{69}\text{H}_{115}\text{N}_{17}\text{O}_{18}\text{Na}_2$, 757.9195, Δ 2.77 ppm).

Pentadecaibin IV (4): white powder, $[\alpha]_{\text{D}}^{20}$ -17.9 (c 1.0, MeOH); UV (MeOH) λ_{max} (log ϵ) 204 (3.42) nm; IR ν_{max} 3304, 2937, 1649, 1531, 1456, 1384, 1361, 1290, 1220, 1176, 1045 cm^{-1} ; ^1H and ^{13}C NMR data, Table S5; ESIMS m/z 764.9 $[\text{M} + 2\text{Na}]^{2+}$, m/z 1506.8 $[\text{M} + \text{Na}]^+$; HRESIMS m/z 764.9263 $[\text{M} + 2\text{Na}]^{2+}$ (calcd for $1/2 \text{C}_{70}\text{H}_{117}\text{N}_{17}\text{O}_{18}\text{Na}_2$, 764.9273, Δ 1.31 ppm).

Pentadecaibin V (5): white powder, $[\alpha]_{\text{D}}^{20}$ -10.2 (c 0.28, MeOH); UV (MeOH) λ_{max} (log ϵ) 204 (3.46) nm; IR ν_{max} 3305, 2933, 1647, 1531, 1455, 1384, 1360, 1288, 1219, 1172, 1043 cm^{-1} ; ^1H and ^{13}C NMR data, Table S6; ESIMS m/z 764.9 $[\text{M} + 2\text{Na}]^{2+}$, m/z 1506.8 $[\text{M} + \text{Na}]^+$; HRESIMS m/z 764.9249 $[\text{M} + 2\text{Na}]^{2+}$ (calcd for $1/2 \text{C}_{70}\text{H}_{117}\text{N}_{17}\text{O}_{18}\text{Na}_2$, 764.9273, Δ 3.14 ppm).

Marfey's Derivatization. Compounds 1–5 (0.5 mg) and 500 μL of 6 M HCl were heated for 24 h at 110 °C in 4 mL sealed tubes (Supelco Analytical; Sigma-Aldrich). Hydrolyzed solutions of peptaibols were evaporated to dryness under a stream of nitrogen and solubilized with 100 μL of H_2O prior to their derivatization with the FDAA Marfey's reagent (Thermo Fisher Scientific). Ten microliters of each aqueous solution of hydrolyzed peptaibol was transferred into a 1 mL HPLC vial, and then 4 μL of 1 M sodium bicarbonate and 20 μL of Marfey's reagent (1% in acetone) were added. The resulting mixture was sealed and then heated at 40 °C for 2 h. After cooling, samples were neutralized with 4 μL of 1 M HCl and diluted 1:3 with MeOH. The same treatment was performed for the Marfey's derivatization of standard AAs (Gly, Aib, D- and L-standards of Glu, Ala, Val, Iva, Leu, and Pheol). Aliquots (10 μL) of hydrolyzed peptaibols and standard AAs were analyzed by HPLC-UV on a reversed-phase analytical column (Inertsil ODS-3 RP18, 250 \times 4.6 mm, 5 μm , Interchim). The elution was ensured at a constant flow rate of 0.5 mL/min using $\text{CH}_3\text{CN}/0.05\%$ TFA in H_2O as mobile phase. The gradient started at 20% CH_3CN ramping up to 50% over

20 min and was then held for 15 min. Detection was performed at 430 nm. All data were acquired by HP ChemStation for LC.

Genome Sequencing and 15-Module NRPS-Encoding Gene Analysis. *Trichoderma* sp. MMS1255 was cultivated in the dark at 25 °C on PDA medium (potato 4 g/L, dextrose 20 g/L, agar 15 g/L, Difco Laboratories). Spore suspensions were produced, and concentrations were adjusted to 10⁷ to 10⁸ spores/mL prior to storage at −80 °C until use. Genomic DNA was extracted from fresh mycelium, following the CTAB method proposed by the Joint Genome Institute with an optional step using Qiagen genome-tips.⁶⁵ The genome was sequenced with PacBio technology. Sequences were quality checked with FastQC.⁶⁶ The genome was assembled using canu.⁶⁷ Secondary metabolism-associated genes (polyketide synthase, PKS; nonribosomal peptide synthetase, NRPS; terpene synthase, TPS; dimethylallyl tryptophan synthase, DMATS) and genes potentially involved in adaptation to the environment were searched in each species. Gene clusters associated with secondary metabolites were searched with FungiSMASH.⁵¹

Cytotoxicity Assays. KB cells (human oral epidermoid carcinoma ATCC CCL 17, American Type Culture Collection) were cultivated in RPMI (Roswell Park Memorial Institute medium) supplemented with 5% (v/v) fetal calf serum, 1% (v/v) glutamine 200 mM, and 1% (v/v) streptomycin (10 mg/mL)/penicillin (1000 U) (all Sigma-Aldrich). Cells were cultivated in plastic flasks (Falcon; Becton Dickinson Labware) at 37 °C in a 5% CO₂-enriched atmosphere. After an incubation period of 48 h, trypsinized cells were suspended as a 2 × 10⁵ cells/mL suspension, and 50 μL was put in each well of 96-well microplates (Nunclon Delta Surface; Thermo Fisher Scientific). After an incubation of 48 h, 50 μL of peptaibol samples was added to the initial 50 μL cell suspension. Peptaibol samples were tested in a well as a final 5% (v/v) methanolic solution in supplemented RPMI with concentrations ranging from 0.6 to 25 μg/mL. A final 5% (v/v) methanolic solution in supplemented RPMI was used as solvent control. Synthetic alamethicin⁵⁵ was used as positive control. After 72 h of incubation, the cell viability was evaluated by the colorimetric 3-(4,5-dimethylthiazol-2-yl)-2,5-diphenyltetrazolium bromide (MTT, Sigma-Aldrich) bioassay.^{68,69}

Antimicrobial Assays. The *C. albicans* clinical isolate was obtained from the Angers University Hospital (Angers, France); *E. coli* (CIP54.8T) and *S. aureus* (CIP53.156) strains are part of the Pasteur Institute Collection. Precultures were inoculated with loopfuls of cells from agar plates and incubated 20 h at the appropriate temperature of 30 °C (for *C. albicans*) or 37 °C (for bacterial strains) on a rotator in 5 mL of YDP medium (yeast dextrose peptone) (for *C. albicans*) or LB medium (Lysogeny Broth) (for bacterial strains). Overnight precultures were then harvested by centrifugation, washed in sterile H₂O, and inoculated to an optical density (OD) of 0.5 in fresh YPD or LB media. The microplate wells were filled with calibrated suspensions and peptaibols to be tested at the desired concentration (ranging from 1 to 100 μg/mL in 1% MeOH, 300 μL/well), and microbial growth was automatically recorded at 600 nm using a multiplate spectrophotometer (Spectrostar Nano; BMG Labtech). The plates were subjected to permanent shaking at 200 rpm, and OD measurements were taken every 10 min during a 24 h period. For each condition, the area under the growth curve representative of the lag phase and the maximal growth rate was calculated as previously described.⁷⁰ A percentage of growth inhibition was calculated for each independent experiment (100 − (AUC_{treated}/AUC_c) × 100 where AUC_{treated} is the area under the growth curve after exposure to the selected peptaibol or antibiotic and AUC_c is the area under the growth curve of an untreated culture). All data presented herein were obtained from two independent biological repetitions, and each repetition included three technical replicates. Amphotericin B (100% inhibition of *C. albicans* at 30 μg/mL in 1% MeOH) and gentamycin (100% inhibition of *E. coli* and *S. aureus* at 40 μg/mL in 1% MeOH) were used as positive controls.

■ ASSOCIATED CONTENT

SI Supporting Information

The Supporting Information is available free of charge at <https://pubs.acs.org/doi/10.1021/acs.jnatprod.0c01355>.

Morphological, genomic and phylogenetic analyses of *Trichoderma* sp. MMS1255, MS and MS² spectra, 1D and 2D NMR spectra, ECD data, and HPLC-UV data for Marfey's analysis of compounds 1–5 (PDF)

■ AUTHOR INFORMATION

Corresponding Author

Nicolas Ruiz – Université de Nantes, MMS - EA2160, 44000 Nantes, France; orcid.org/0000-0001-7330-4679; Phone: +33 (0)2 53 48 41 96; Email: nicolas.ruiz@univ-nantes.fr; Fax: +33 (0)2 53 48 41 09

Authors

Anne-Isaline van Bohemen – Université de Nantes, MMS - EA2160, 44000 Nantes, France

Aurore Zalouk-Vergnoux – Université de Nantes, MMS - EA2160, 44000 Nantes, France

Aurore Michaud – Université de Nantes, MMS - EA2160, 44000 Nantes, France

Thibaut Robiou du Pont – Université de Nantes, MMS - EA2160, 44000 Nantes, France

Irina Druzhinina – Institute of Chemical, Environmental and Bioscience Engineering, TU Wien, 1040 Vienna, Austria; Fungal Genomics Laboratory (FungiG), Nanjing Agricultural University, 210095 Nanjing, China

Lea Atanasova – Department of Food Science and Technology, University of Natural Resources and Life Sciences – BOKU, 1190 Vienna, Austria

Soizic Prado – Muséum National d'Histoire Naturelle, Unité Molécules de Communication et Adaptation des Micro-organismes, 75005 Paris, France

Bernard Bodo – Muséum National d'Histoire Naturelle, Unité Molécules de Communication et Adaptation des Micro-organismes, 75005 Paris, France

Laurence Meslet-Cladiere – Université de Brest, Laboratoire Universitaire de Biodiversité et Ecologie Microbienne, 29280 Plouzané, France

Bastien Cochereau – Université de Nantes, MMS - EA2160, 44000 Nantes, France; Université de Brest, Laboratoire Universitaire de Biodiversité et Ecologie Microbienne, 29280 Plouzané, France

Franck Bastide – IRHS-UMR1345, Université d'Angers, INRAE, Institut Agro, 49071 Beaucouzé, France

Corentin Maslard – IRHS-UMR1345, Université d'Angers, INRAE, Institut Agro, 49071 Beaucouzé, France

Muriel Marchi – IRHS-UMR1345, Université d'Angers, INRAE, Institut Agro, 49071 Beaucouzé, France

Thomas Guillemette – IRHS-UMR1345, Université d'Angers, INRAE, Institut Agro, 49071 Beaucouzé, France

Yves François Pouchus – Université de Nantes, MMS - EA2160, 44000 Nantes, France

Complete contact information is available at:

<https://pubs.acs.org/10.1021/acs.jnatprod.0c01355>

Notes

The authors declare no competing financial interest.

ACKNOWLEDGMENTS

This work was supported by a Ph.D. grant for A.I.V.B. from the French Ministry of Higher Education and Research. The authors acknowledge the French Ministry of Agriculture and Food for the research program NABUCO (Ecophyto 2 plan). The 600 MHz NMR spectrometer used in this study was funded jointly by the Région Ile-de-France, the Museum National d'Histoire Naturelle (Paris, France), and CNRS (France). Dr. A. Blond is gratefully acknowledged for recording the NMR spectra. The authors also thank Dr. M. Chollet-Krugler (COInt, University of Rennes) for specific rotation measurements, A. Tonnerre (IICIMed, University of Nantes) for IR spectroscopy, and Prof. F. Fleury (IMPACT platform, Biogenouest, University of Nantes) for ECD experiments. We also gratefully acknowledge Dr. Y. Fichou (ESC Bretagne Brest) for the PacBio sequencing, Dr. A. Lebreton and Dr. E. Corre (Roscoff Marine Station, Sorbonne Univeristy) for their help in the genome assembly, and Prof. N. Inguibert (CRIOBE, University of Perpignan Via Domitia) for providing synthetic alamethicin F50/S.

REFERENCES

- (1) Chugh, J. K.; Wallace, B. A. *Biochem. Soc. Trans.* **2001**, *29* (4), 565–570.
- (2) Degenkolb, T.; Berg, A.; Gams, W.; Schlegel, B.; Gräfe, U. *J. Pept. Sci.* **2003**, *9* (11–12), 666–678.
- (3) Degenkolb, T.; Brückner, H. *Chem. Biodiversity* **2008**, *5* (9), 1817–1843.
- (4) Degenkolb, T.; Kirschbaum, J.; Brückner, H. *Chem. Biodiversity* **2007**, *4* (6), 1052–1067.
- (5) Mukherjee, P. K.; Wiest, A.; Ruiz, N.; Keightley, A.; Moran-Diez, M. E.; McCluskey, K.; Pouchus, Y. F.; Kenerley, C. M. *J. Biol. Chem.* **2011**, *286*, 4544–4554.
- (6) Reiber, K.; Neuhof, T.; Ozegowski, J. H.; Von Döhren, H.; Schwecke, T. *J. Pept. Sci.* **2003**, *9*, 701–713.
- (7) Wiest, A.; Grzegorski, D.; Xu, B. W.; Goulard, C.; Rebuffat, S.; Ebbole, D. J.; Bodo, B.; Kenerley, C. *J. Biol. Chem.* **2002**, *277* (23), 20862–20868.
- (8) Neumann, N. K. N.; Stoppacher, N.; Zeilinger, S.; Degenkolb, T.; Brückner, H.; Schuhmacher, R. *Chem. Biodiversity* **2015**, *12* (5), 743–751.
- (9) Stoppacher, N.; Neumann, N. K. N.; Burgstaller, L.; Zeilinger, S.; Degenkolb, T.; Brückner, H.; Schuhmacher, R. *Chem. Biodiversity* **2013**, *10* (5), 734–743.
- (10) Duchohier, H. *Chem. Biodiversity* **2007**, *4* (6), 1023–1026.
- (11) Shi, M.; Wang, H. N.; Xie, S. T.; Luo, Y.; Sun, C. Y.; Chen, X. L.; Zhang, Y. Z. *Mol. Cancer* **2010**, *9* (1), 26.
- (12) Oh, S. U.; Yun, B. S.; Lee, S. J.; Kim, J. H.; Yoo, I. D. *J. Antibiot.* **2002**, *55* (6), 557–564.
- (13) Su, H. N.; Chen, Z. H.; Song, X. Y.; Chen, X. L.; Shi, M.; Zhou, B. C.; Zhao, X.; Zhang, Y. Z. *PLoS One* **2012**, *7* (9), e45818.
- (14) Summers, M. Y.; Kong, F.; Feng, X.; Siegel, M. M.; Janso, J. E.; Graziani, E. I.; Carter, G. T. *J. Nat. Prod.* **2007**, *70* (3), 391–396.
- (15) Ayers, S.; Ehrmann, B. M.; Adcock, A. F.; Kroll, D. J.; Carcache de Blanco, E. J.; Shen, Q.; Swanson, S. M.; Falkinham, J. O.; Wani, M. C.; Mitchell, S. M.; Pearce, C. J.; Oberlies, N. H. *J. Pept. Sci.* **2012**, *18* (8), 500–510.
- (16) Pruksakorn, P.; Arai, M.; Kotoku, N.; Vilchèze, C.; Baughn, A. D.; Moodley, P.; Jacobs Jr, W. R.; Kobayashi, M. *Bioorg. Med. Chem. Lett.* **2010**, *20* (12), 3658–3663.
- (17) Pruksakorn, P.; Arai, M.; Liu, L.; Moodley, P.; Jacobs, W. R., Jr.; Kobayashi, M. *Biol. Pharm. Bull.* **2011**, *34* (8), 1287–1290.
- (18) Touati, I.; Ruiz, N.; Druzhinina, I.; Atanasova, L.; Tabenne, O.; Elkahoui, S.; Benzekri, R.; Bouslama, L.; Pouchus, Y. F.; Liman, F. *World J. Microbiol. Biotechnol.* **2018**, *34* (98), 1–12.
- (19) Song, X. Y.; Shen, Q. T.; Xie, S. T.; Chen, X. L.; Sun, C. Y.; Zhang, Y. Z. *FEMS Microbiol. Lett.* **2006**, *260* (1), 119–125.
- (20) Luo, Y.; Zhang, D. D.; Dong, X. W.; Zhao, P. B.; Chen, L. L.; Song, X. Y.; Wang, X. J.; Chen, X. L.; Shi, M.; Zhang, Y. Z. *FEMS Microbiol. Lett.* **2010**, *313* (2), 120–126.
- (21) Kim, Y. H.; Yeo, W. H.; Kim, Y. S.; Chae, S. Y.; Kim, K. S. *J. Microbiol. Biotechnol.* **2000**, *10* (4), 522–528.
- (22) Yun, B. S.; Yoo, I. D.; Kim, Y. H.; Kim, Y. S.; Lee, S. J.; Kim, K. S.; Yeo, W. H. *Tetrahedron Lett.* **2000**, *41* (9), 1429–1431.
- (23) El Hajji, M.; Rebuffat, S.; Le Doan, T.; Klein, G.; Satre, M.; Bodo, B. *Biochim. Biophys. Acta, Biomembr.* **1989**, *978* (1), 97–104.
- (24) Nagaraj, G.; Uma, M. V.; Shivayogi, M. S.; Balaran, H. *Antimicrob. Agents Chemother.* **2001**, *45* (1), 145–149.
- (25) Otto, A.; Laub, A.; Wendt, L.; Porzel, A.; Schmidt, J.; Palfner, G.; Becerra, J.; Krüger, D.; Stadler, M.; Wessjohann, L.; Westermann, B.; Arnold, N. *J. Nat. Prod.* **2016**, *79* (4), 929–938.
- (26) Degenkolb, T.; Nielsen, K. F.; Dieckmann, R.; Branco-Rocha, F.; Chaverri, P.; Samuels, G. J.; Thrane, U.; von Döhren, H.; Vilcinskis, A.; Brückner, H. *Chem. Biodiversity* **2015**, *12* (4), 662–684.
- (27) Shi, M.; Chen, L. L.; Wang, X. W.; Zhang, T.; Zhao, P. B.; Song, X. Y.; Sun, C. Y.; Chen, X. L.; Zhou, B. C.; Zhang, Y. Z. *Microbiology* **2012**, *158*, 166–175.
- (28) Viterbo, A.; Wiest, A.; Brotman, Y.; Chet, I.; Kenerley, C. *Mol. Plant Pathol.* **2007**, *8* (6), 737–746.
- (29) Béven, L.; Duval, D.; Rebuffat, S.; Riddell, F. G.; Bodo, B.; Wróblewski, H. *Biochim. Biophys. Acta, Biomembr.* **1998**, *1372* (1), 78–90.
- (30) Mohamed-Benkada, M.; François Pouchus, Y.; Vérité, P.; Pagniez, F.; Caroff, N.; Ruiz, N. *Chem. Biodiversity* **2016**, *13* (5), 521–530.
- (31) Carroux, A.; Van Bohemen, A. I.; Roullier, C.; Robiou du Pont, T.; Vansteelandt, M.; Bondon, A.; Zalouk-Vergnoux, A.; Pouchus, Y. F.; Ruiz, N. *Chem. Biodiversity* **2013**, *10* (5), 772–786.
- (32) Ruiz, N.; Wielgosz-Collin, G.; Poirier, L.; Grovel, O.; Petit, K. E.; Mohamed-Benkada, M.; Robiou du Pont, T.; Bissett, J.; Vérité, P.; Barnathan, G.; Pouchus, Y. F. *Peptides* **2007**, *28* (7), 1351–1358.
- (33) Landreau, A.; Pouchus, Y. F.; Sallenave-Namont, C.; Biard, J. F.; Boumard, M. C.; Robiou du Pont, T.; Mondeguer, F.; Goulard, C.; Verbist, J. F. *J. Microbiol. Methods* **2002**, *48* (2–3), 181–194.
- (34) Chaverri, P.; Branco-Rocha, F.; Jaklitsch, W. M.; Gazis, R. O.; Degenkolb, T.; Samuels, G. J. *Mycologia* **2015**, *107* (3), 558–590.
- (35) Jaklitsch, W. M.; Voglmayr, H. *Mycotaxon* **2013**, *126* (1), 143–156.
- (36) Druzhinina, I. S.; Kubicek, C. P.; Komoń-Zelazowska, M.; Mulaw, T. B.; Bissett, J. *BMC Evol. Biol.* **2010**, *10* (1), 94.
- (37) Taylor, J. W.; Jacobson, D. J.; Kroken, S.; Kasuga, T.; Geiser, D. M.; Hibbett, D. S.; Fisher, M. C. *Fungal Genet. Biol.* **2000**, *31* (1), 21–32.
- (38) Kumar, S.; Stecher, G.; Tamura, K. *Mol. Biol. Evol.* **2016**, *33* (7), 1870–1874.
- (39) Hosotani, N.; Kumagai, K.; Honda, S.; Ito, A.; Shimatani, T.; Saji, I. *J. Antibiot.* **2007**, *60* (3), 184–190.
- (40) Rebuffat, S.; Goulard, C.; Bodo, B. *J. Chem. Soc., Perkin Trans. I* **1995**, 1849–1855.
- (41) Toniolo, C.; Polese, A.; Formaggio, F.; Crisma, M.; Kamphuis, J. *J. Am. Chem. Soc.* **1996**, *118* (11), 2744–2745.
- (42) De Zotti, M.; Schievano, E.; Mammi, S.; Kaptein, B.; Broxterman, Q. B.; Singh, S. B.; Brückner, H.; Toniolo, C. *Chem. Biodiversity* **2010**, *7* (6), 1612–1624.
- (43) De Zotti, M.; Biondi, B.; Crisma, M.; Hjørringgaard, C. U.; Berg, A.; Brückner, H.; Toniolo, C. *Biopolymers* **2012**, *98* (1), 36–49.
- (44) Bhushan, R.; Brückner, H. *Amino Acids* **2004**, *27* (3), 231–247.
- (45) Ritzau, M.; Heinze, S.; Dornberger, K.; Berg, A.; Fleck, W.; Schlegel, B.; Härtl, A.; Gräffe, U. *J. Antibiot.* **1997**, *50* (9), 722–728.
- (46) Lee, S. J.; Yun, B. S.; Cho, D. H.; Yoo, I. D. *J. Antibiot.* **1999**, *52* (11), 998–1006.
- (47) Kronen, M.; Kleinwachter, P.; Schlegel, B.; Hartl, A.; Grafe, U. *J. Antibiot.* **2001**, *54* (2), 175–178.

- (48) Neuhof, T.; Berg, A.; Besl, H.; Schwecke, T.; Dieckmann, R.; von Dohren, H. *Chem. Biodiversity* **2007**, *4* (6), 1103–1115.
- (49) Berek, I.; Becker, A.; Schröder, H.; Härtl, A.; Höllt, V.; Grecksch, G. *Behav. Brain Res.* **2009**, *203* (2), 232–239.
- (50) Grigoriev, I. V.; Nikitin, R.; Haridas, S.; Kuo, A.; Ohm, R.; Otilar, R.; Riley, R.; Salamov, A.; Zhao, X.; Korzeniewski, F.; Smirnova, T.; Nordberg, H.; Dubchak, I.; Shabalov, I. *Nucleic Acids Res.* **2014**, *42* (D1), D699–D704.
- (51) Blin, K.; Shaw, S.; Steinke, K.; Villebro, R.; Ziemert, N.; Lee, S. Y.; Medema, M. H.; Weber, T. *Nucleic Acids Res.* **2019**, *47* (W1), W81–W87.
- (52) Manavalan, B.; Murugapiran, S. K.; Lee, G.; Choi, S. *BMC Struct. Biol.* **2020**, *10* (1), 1.
- (53) Rausch, C.; Weber, T.; Kohlbacher, O.; Wohlleben, W.; Huson, D. H. *Nucleic Acids Res.* **2005**, *33* (18), 5799–5808.
- (54) Röttig, M.; Medema, M. H.; Blin, K.; Weber, T.; Rausch, C.; Kohlbacher, O. *Nucleic Acids Res.* **2011**, *39*, W362–W367.
- (55) Ben Haj Salah, K.; Inguibert, N. *Org. Lett.* **2016**, *16* (6), 1783–1785.
- (56) Das, S.; Ben Haj Salah, K.; Wenger, E.; Martinez, J.; Kotarba, J.; Andreu, V.; Ruiz, N.; Savini, F.; Stella, L.; Didierjean, C.; Legrand, B.; Inguibert, N. *Chem. Eur. J.* **2017**, *23* (71), 17964–17972.
- (57) Jiao, W. H.; Khalil, Z.; Dewapriya, P.; Salim, A. A.; Lin, H. W.; Capon, R. J. *J. Nat. Prod.* **2018**, *81* (4), 976–984.
- (58) Goodwin, D. C.; Lee, S. B. *Biotechniques* **1993**, *15* (3), 438–444.
- (59) Carbone, I.; Kohn, L. M. *Mycologia* **1999**, *91* (3), 553–556.
- (60) White, T. J.; Bruns, T. D.; Lee, S.; Taylor, J. In *PCR Protocols: A Guide to Methods and Applications*; Innis, M. A.; Gelfand, D. H.; Sninsky, J. J.; White, T. J., Eds.; Academic Press: London, 1990; pp 315–322.
- (61) Liu, Y. J.; Whelen, S.; Hall, B. D. *Mol. Biol. Evol.* **1999**, *16* (12), 1799–1808.
- (62) Jaklitsch, W. M.; Komon, M.; Kubicek, C. P.; Druzhinina, I. S. *Mycologia* **2005**, *97* (6), 1365–1378.
- (63) Hall, T. A. *Nucleic Acids Symp. Ser.* **1999**, *41*, 95–98.
- (64) Rodríguez, F.; Oliver, J. L.; Marin, A.; Medina, J. R. *J. Theor. Biol.* **1990**, *142* (4), 485–501.
- (65) Kohler, A.; Murat, C.; Costa, M. High quality genomic DNA extraction using CTAB and Qiagen genomic-tip. Version 2. INRA Nancy Equipe Ecogénomique UMR Iam, 2011. <http://1000.fungalgenomes.org/home/wp-content/uploads/2013/02/genomicDNAProtocol-AK0511.pdf> (accessed April 15, 2020).
- (66) Andrews, S. FastQC: A quality control tool for high throughput sequence data, 2010. <http://www.bioinformatics.babraham.ac.uk/projects/fastqc/> (accessed April 15, 2020).
- (67) Koren, S.; Walenz, B. P.; Berlin, K.; Miller, J. R.; Bergman, N. H.; Phillippy, A. M. *Genome Res.* **2017**, *27* (5), 722–736.
- (68) Denizot, F.; Lang, R. J. *J. Immunol. Methods* **1986**, *89* (2), 271–277.
- (69) Mosman, N. T. J. *J. Immunol. Methods* **1983**, *65*, 55–63.
- (70) Gaucher, M.; Dugé de Bernonville, T.; Lohou, D.; Guyot, S.; Guillemette, T.; Brisset, M. N.; Dat, J. F. *Phytochemistry* **2013**, *90*, 78–89.